Hyperfine Interactions 123/124 (1999) 595–609

Diffusion in crystalline materials

G. Vogl and B. Sepiol

Institut für Materialphysik der Universität Wien, Strudlhofgasse 4, A-1090 Wien, Austria

Recently nuclear scattering of synchrotron radiation proved to be a powerful new method to study the elementary diffusion jump in crystalline solids. The scattered radiation decays faster when atoms move on the time scale of the excited-state lifetime of a Mössbauer isotope because of a loss of coherence. The acceleration of the decay rate differs for different crystal orientations relative to the beam providing information not only about the rates but also about the directions of the elementary jumps. We discuss first applications of the method.

1. Introduction

1.1. Diffusion in crystalline materials

There is no need to emphasize the importance of diffusion for innumerable processes in materials, quasi-continuous (gases, liquids, glasses) or with discrete structure, i.e., crystalline solids. Fick was the first to formulate a law of diffusion, thinking of continuous media. It is most remarkable that for a long time no methods were available for detecting atomic jumps between well-defined residence sites in solids in an atomistic way, i.e., to determine the elementary diffusion jumps, which implies determining jump frequency and jump vector. Nearly all information on the mechanism of diffusion was derived in a rather indirect way from studies of radiotracer diffusion which is a bulk phenomenon of great sensitivity, lacking, however, any atomistic information. Some relaxation methods allowed one to deduce a jump frequency, tacitly taking for granted that these jumps exist, but the jump vector, i.e., length and direction of the diffusion jumps, remained unknown.

1.2. Atomistic methods, in particular nuclear resonant scattering of synchrotron radiation

We confine ourselves in this paper to diffusion processes where indeed the full information on jump frequency and vector is necessary to describe the event, i.e., we limit this paper to diffusion in crystalline materials. For diffusion in glasses see the contribution by Franz et al. [1].

The breakthrough of quasielastic neutron scattering (QNS), promoted by Brockhouse in the late fifties [2], opened the way to an atomistic view on diffusion. Quasielastic Mössbauer spectroscopy (QMS) on diffusion started in the late sixties [3], after

the theoretical papers by Singwi and Sjölander on how to study diffusion in solids with QNS and QMS [4]. In the case of QNS, diffusion manifests itself through the energy broadening of the scattered intensity; in the case of QMS, through the analogous broadening of the nuclear resonance line(s).

In the following we explain how to use the new technique of nuclear resonant scattering of synchrotron radiation [5–7] for studying diffusion directly in the time domain, whereas QMS and QNS studies work in the energy domain.

In this paper we shall mainly discuss nuclear resonant forward scattering of synchrotron radiation. NRS is, however, not limited to scattering in the forward direction and some preliminary results obtained for scattering into the Bragg directions will also be presented.

The principal idea of NRS is: the extreme coherence of the SR in the forward direction (the phase matching) after nuclear resonance absorption in the sample is destroyed by diffusion through "muddling up" the phases of the partial wave trains reemitted from the jumping atoms. This leads to a faster decay of the intensity of the reemitted radiation. From this *diffusionally accelerated decay*, details on the diffusion process can be derived, in particular when the sample is a single crystal.

2. A few words about theory

Here we give only an outline, for more details see the contribution by Kohn and Smirnov in this issue (section III-1.5).

2.1. Scattering functions for diffusion

All nuclear methods have common principles, essentially already described in the original theory of Singwi and Sjölander about the effects of diffusion on quasielastic neutron scattering (QNS) and quasielastic Mössbauer spectroscopy (QMS) [3]. The diffusion is contained in the intermediate scattering function[1] $I(\mathbf{Q}, t)$ which is a Fourier transform of the diffusional part of the space–time self-correlation function $G(\mathbf{r}, t)$:

$$I(\mathbf{Q}, t) = \int \mathrm{d}\mathbf{r}\ \exp(-\mathrm{i}\mathbf{Q}\mathbf{r})\, G_S(\mathbf{r}, t), \tag{2.1}$$

where $\mathbf{Q}$ is the momentum transfer from/to the interacting radiation.

In the following we perform the usual separation into the slow diffusional motions and the much faster lattice vibration. The energy change (the phonons) which the lattice vibrations transfer to the radiation is far out of the energy window of interest in diffusion studies; therefore lattice vibrations are only of interest here inasmuch as they

[1] The name "intermediate" is derived originally from QNS where the measured scattering function $S(\mathbf{Q}, \omega)$ is calculated from the space–time correlation function $G(\mathbf{r}, t)$ by performing first a Fourier transform from space into momentum (leading to the *intermediate* scattering function) and then a Fourier transformation from time into energy, leading to $S(\mathbf{Q}, \omega)$.

cause an intensity reduction of the quasielastic radiation through the Lamb–Mössbauer factor.

For Markovian diffusion on crystalline lattices of Bravais type (i.e., only one sublattice) the intermediate scattering function is simply an exponential of time, modulated by the lattice structure [8]:

$$I(\mathbf{Q},t) = \exp\left[-\frac{t}{\tau}\sum_{i=1}^{N} N^{-1}\left\{1-\exp(-\mathrm{i}\mathbf{Q}\mathbf{l}_i)\right\}\right] = \exp\left[-\frac{t}{\tau}\alpha(\mathbf{Q})\right], \qquad (2.2)$$

with τ the residence time on one site (its reciprocal being the jump frequency to any neighbour site). The diffusion jumps follow jump vectors $\mathbf{l}_i$ to N possible sites. In the simplest case of jumps to nearest neighbours (NN) only, i counts the NNs from 1 to their number N.

The right hand side of eq. (2.2) is an abbreviated form defining $\alpha(\mathbf{Q})$, which describes the summation of partial wave trains when the atom jumps from site to site on what we may call the "jump lattice", i.e., the ensemble of neighbour sites reached by jumps during the interaction time with the probing radiation. We call $\alpha(\mathbf{Q})$ the "jump function" because it contains all information on the sites visited by a jumping atom during the interaction time.

From $I(\mathbf{Q},\mathbf{t})$, the universal resonance function $\varphi(\mathbf{Q},\omega)$ [9] is calculated by a time-to-energy Laplace transformation

$$\varphi(\mathbf{Q},\omega) = \int_0^\infty \mathrm{d}t \exp\left[\mathrm{i}\omega t - \frac{\Gamma_0 t}{2\hbar}\right] I(\mathbf{Q},t), \qquad (2.3)$$

where for NRS and QMS Γ_0 is the natural width (FWHM) of the excited state of the nucleus, for QNS it is the experimental resolution if we regard it as having approximately a Lorentzian distribution.

By the integration one obtains

$$\varphi(\mathbf{Q},\omega) = \mathrm{i}\left\{\omega + \mathrm{i}\left[\left(\frac{\Gamma_0}{2\hbar}\right) + \frac{1}{\tau}\,\alpha(\mathbf{Q})\right]\right\}^{-1}. \qquad (2.4)$$

In the two "old" methods, QMS and QNS, the *real part* of $\varphi(\mathbf{Q},\omega)$ is the essential factor of the absorption cross section and the emission probability and of the scattering function. $(2\hbar/\tau)\alpha(\mathbf{Q})$ is equal to $\Gamma_d(\mathbf{Q})$, the energy width (FWHM) caused by diffusion, responsible for the Lorentzian shaped "diffusional line broadening".

In nuclear resonant scattering of synchrotron radiation, in particular, in nuclear forward scattering, $\varphi(\mathbf{Q},\omega)$ describes the dynamical effects on the spectrum, which consist of a time-accelerated decay of the scattered intensity because the coherency among the partial wave trains from the different diffusion sites is destroyed. As already mentioned in section 1, this leads to a "diffusionally accelerated" decay of the coherently forward scattered intensity.

2.2. Diffusion and nuclear resonant forward scattering

As just mentioned, $\varphi(\mathbf{Q},\omega)$ describes diffusional effects on the spectrum. In the case of a *thin sample* the intensity[2] $I_{\mathrm{FS}}(\mathbf{Q},t)$ of nuclear resonant scattering in the *forward direction* in the presence of diffusion can be expressed directly by the intermediate scattering function $I(\mathbf{Q},t)$ [10] leaving out the mathematically abstract transformation into the energy domain, as is necessary for QMS and QNS:

$$I_{\mathrm{FS}}(\mathbf{Q},t) = I_0\left(\frac{L^2}{4\tau_0}\right)\exp\left(-\frac{t}{\tau_0}\right)\left|I(\mathbf{Q},t)\right|^2, \tag{2.5}$$

where I_0 is the fraction of incoming radiation within the width of the nulear level (in the following the 14.4 keV level of ^{57}Fe) reduced by electronic absorption in the sample, t is the time after nuclear excitation by the synchrotron pulse, L is the "effective sample thickness", which is the product of the number of scattering atoms in the sample, the nuclear absorption cross section and (relevant in solid state investigation) the Lamb–Mössbauer factor. τ_0 is the natural lifetime of the nucleus (141 ns for ^{57}Fe).

We mention here (but for sake of simplicity shall not elaborate that general case in detail) that for finite sample thickness the expression for the intensity of nuclear forward scattering is considerably less lucid (for details, see [10]):

$$I_{\mathrm{FS}}(\mathbf{Q},t) = I_0(2\pi)^{-1}\left|\int_{-\infty}^{+\infty}\mathrm{d}\omega\exp(-\mathrm{i}\omega t)\exp\left[-\frac{L}{4\tau_0}\,\varphi(\mathbf{Q},\omega)\right]\right|^2. \tag{2.6}$$

2.3. Diffusion and non-forward scattering

For scattering in *other directions* than forward, we must distinguish several cases.

2.3.1. Resonant incoherent scattering

Up to now experiments on the influence of diffusion on nuclear resonant scattering have treated without exception the accelerated decay of the forward scattered intensity. Because resonant scattering is a nuclear process, which cannot be directly affected by atomic motions, one would expect this fraction to go somewhere else. Since the reason for the intensity drop in the forward direction is the destruction of coherence by nuclei that change their sites during nuclear excitation, it is obvious that the missing intensity will be scattered incoherently in all directions [9]. Of course, it is more difficult to measure this diffuse part than the forward coherent intensity, which is the reason why only exceptionally such experiments have been performed so far [11]. An attempt to measure the dynamical effects through incoherent scattering of synchrotron radiation was performed on a glass [12] but the inelastic background was too large to observe the slower intensity decay predicted by [9].

[2] In order to gain maximum information about the jumps, the samples have to be single crystals. In forward scattering the vector $\mathbf{Q}$ is fixed, its length being 7.3 Å^{-1}, but the angles of the jump vectors $\mathbf{l}_i$ versus $\mathbf{Q}$ can be varied by changing the crystal orientation. We symbolise this dependence by writing $I_{\mathrm{FS}}(\mathbf{Q},t)$.

2.3.2. Resonant Bragg-scattering

For crystalline materials the phenomenon of coherent scattering should not only be observable in the forward direction, but also for all momentum transfers that fulfill the Bragg-condition $\Delta\mathbf{Q} = \mathbf{G}$, where $\mathbf{G}$ is a reciprocal lattice vector. Of course, this condition restricts the possibility of observing accelerated decay of coherent intensity to a limited number of directions, on the other hand this technique allows us to work in a scattering geometry which permits the use of thick samples which cannot be prepared as thin foils due to their brittleness. Feasibility tests on Fe_3Si single crystals were performed very recently [13].

2.3.3. Rayleigh scattering

Rayleigh scattering, i.e., elastic scattering from the electronic shells of the atom, of radiation which has undergone nuclear resonant scattering before reaching the sample, allows the study of samples without ^{57}Fe or other Mössbauer isotopes. This method will hopefully lift the restrictions to very few Mössbauer isotopes and in fact allow for diffusion studies at high temperatures. Rayleigh scattering is a fully coherent process, in consequence one observes the coherent scattering function $S(\mathbf{Q}, \omega)$ which is the Fourier transformed pair-correlation-function $G(\mathbf{r}, t)$. There have been attempts to use nuclear resonant monochromators like $^{57}FeBO_3$ [14] to provide a time-independent high-brilliance source of Mössbauer quanta, which could be scattered by the sample and analyzed by using a Doppler-shifted absorber to obtain $S(\mathbf{Q}, \omega)$. Unfortunately, this is a difficult task due to the complicated hyperfine structure of $FeBO_3$.

A more direct way of measuring atomic diffusion consists of observing in the time domain the decay of quantum beats, produced by resonant scattering of synchrotron radiation on two stainless-steel foils in constant relative motion, one in front of the sample, the other behind the sample. The method is called time domain interferometry [15] and can again be related to the pair correlation function via $I(\mathbf{Q}, t) \propto \int \mathrm{d}r \exp(-\mathrm{i}\mathbf{Q}\mathbf{r})\, G(\mathbf{r}, t)$. In crystalline materials the scattered intensity is mainly found in Bragg reflections, which restricts the measurement of $I(\mathbf{Q}, t)$ to a few singular points in reciprocal space, except for disordered samples where additional Laue monotonic scattering provides more or less isotropic intensity. According to the recently published theory of Ruebenbauer [16] this method will allow the investigation of the atomistic diffusion mechanism beyond iron.

3. Experiments on forward scattering

We shall explain the potential of NRS for studying diffusion in crystalline materials for two examples.

Experiments with NRS were carried out at the nuclear resonance beamline of the ESRF (for details on the beam line see [17]). The storage ring operated in 16-bunch mode providing short pulses of X-rays (duration about 100 ps) every 176 ns. The radiation from the undulator source, optimized for the 14.4 keV transition in iron, was filterd by a double Si (1 1 1) reflection followed by monochromatization in a high

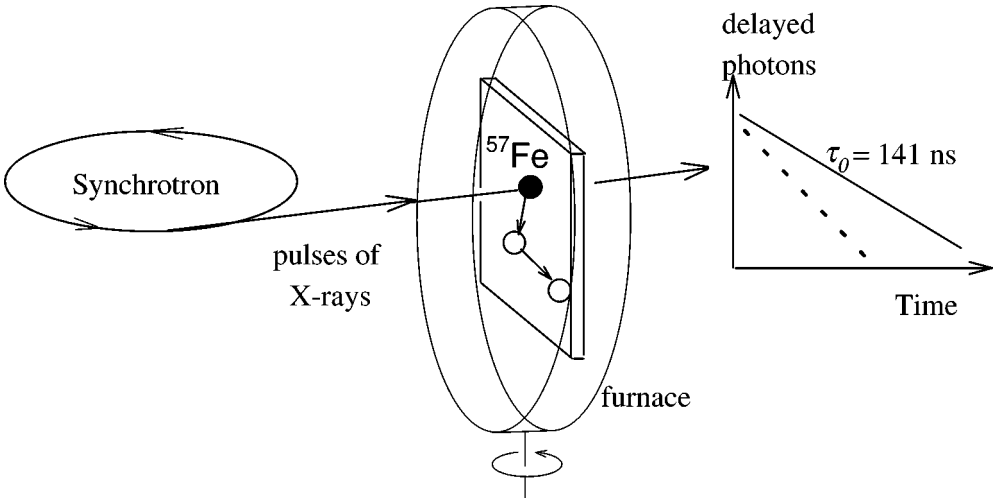

Figure 1. Set-up used in investigations of diffusion with nuclear resonant forward scattering. The crystal orientation relative to the synchrotron beam can be freely chosen.

resolution nested monochromator. The delayed events, resulting from nuclear forward scattering, were counted by a fast avalanche photodiode (APD) detector. Because of overloading of the detector immediately after the synchrotron pulse, data taken during the first 20–25 ns after each pulse had to be discarded.

The samples were heated in a furnace which was mounted on a goniometer head permitting orientation of the furnace together with the sample relative to the synchrotron beam. Temperatures up to 1100 °C are possible. Encapsulation of the samples (in BN or in BeO ceramics) is necessary in order to prevent crumbling and evaporation at high temperatures. Figure 1 shows schematically the set-up of a diffusion experiment with NRS. The crystals were sufficiently thin (in the order of 20 μm) to allow the thin sample approximation. To obtain the intensity in forward scattering in a crystalline sample, we insert eq. (2.1) into eq. (2.5):

$$I_{\mathrm{FS}}(\mathbf{Q},t) = I_0\,\frac{L^2}{4\tau_0}\exp\!\left(-\frac{t}{\tau_0}\right)\exp\!\left[-\frac{2t}{\tau}\,\alpha(\mathbf{Q})\right]. \tag{3.1}$$

In the case of crystalline lattices of Bravais type, the diffusionally accelerated decay of nuclear scattering in the forward direction can be connected to the natural Mössbauer broadening Γ_0 and the diffusional Mössbauer line width Γ_{d},

$$\Gamma_0 = \frac{\hbar}{\tau_0} \quad \text{and} \quad \Gamma_{\mathrm{d}}(\mathbf{Q}) = \frac{2\hbar}{\tau}\,\alpha(\mathbf{Q}), \tag{3.2}$$

in the following way:

$$I_{\mathrm{FS}}(\mathbf{Q},t) = I_0\,\frac{L^2}{4\tau_0}\exp\!\left[\frac{-t(\Gamma_0+\Gamma_{\mathrm{d}}(\mathbf{Q}))}{\hbar}\right]. \tag{3.3}$$

We see that the logarithm of the decay rate is now proportional to the width of the diffusionally broadened line ($\Gamma_0 + \Gamma_d$), as measured in classical QMS. This has been used in [18] and recently derived more strictly in [10].

3.1. Iron diffusion in FeAl

3.1.1. Time dependence

A system of general interest for diffusion studies was selected as one of the first candidates to test the new method of NRS. It was an intermetallic alloy with the ordered B2 structure (CsCl structure). There, an intriguing question is still under discussion, i.e., whether the atoms of one type, here Fe, jump directly to sites on the Bravais lattice occupied only by Fe atoms, or whether they take the opportunity of the shorter jumps to intermediate residence sites on the Al sublattice.

A crystal of a stoichiometric (equiatomic) sample of the ordered alloy FeAl was oriented with its $(1\,\bar{1}\,1)$-plane horizontal (i.e., in the plane of the synchrotron beam), so that any crystal direction from [1 1 3] through [1 1 1] to [1 1 0] could be adjusted parallel to the beam. Figure 2 shows the time dependence of $I_{\mathrm{FS}}(\mathbf{Q}, t)$ at

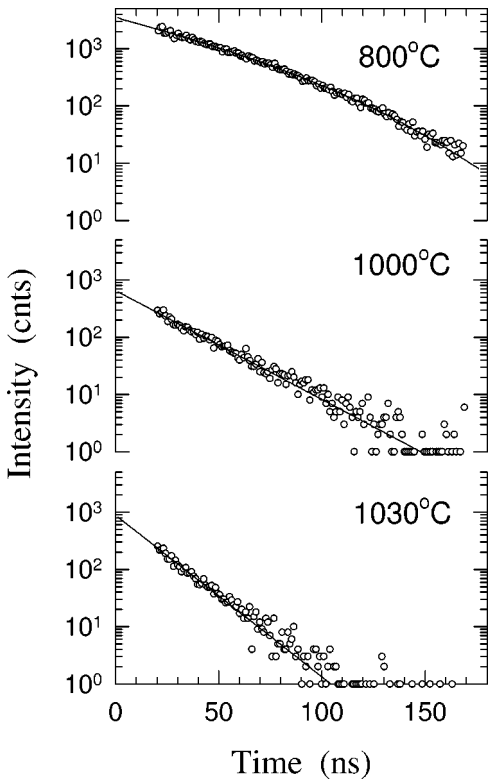

Figure 2. FeAl. Time dependence of forward scattering intensity at three temperatures with the beam parallel to the [1 1 0] crystal direction.

three different temperatures with the beam parallel to the [1 1 0] crystal direction. It is evident that at *high temperatures* the time dependence of the logarithm of the forward scattered intensity indeed follows eq. (3.3), its slope, if measured as a function of crystal orientation, yielding the details of the jump mechanism, i.e., jump frequency and jump vector. At low temperatures, however, the logarithm of the decay deviates from a linear dependence. Here the thin-sample approximation is no longer valid because the Lamb–Mössbauer factor contained in the effective thickness L is too large. Now the full theory has to be applied, i.e., eq. (2.6). For jump diffusion between lattice sites we get [9]

$$I_{\mathrm{FS}}(\mathbf{Q},t) = I_0\,\frac{L}{4t}\,J_1^2\big(\sqrt{Lt/\tau_0}\,\big)\,\exp\!\left[-\frac{t}{\tau}\,\alpha(\mathbf{Q})\right], \tag{3.4}$$

with J_1 the first order Bessel function. In terms of Mössbauer line width:

$$I_{\mathrm{FS}}(\mathbf{Q},t) = I_0\,\frac{L}{4t}\,J_1^2\big(\sqrt{Lt/\tau_0}\,\big)\,\exp\!\left[-\frac{t(\Gamma_0+\Gamma_{\mathrm{d}}(\mathbf{Q}))}{\hbar}\right]. \tag{3.5}$$

For a sufficiently thin sample the Bessel function J_1 can be expanded up to first order and eqs. (3.4) and (3.5) reduce to the simpler eqs. (3.1) and (3.3), respectively. Since diffusional effects are only visible at high temperatures, we shall not discuss the complicated full-theory case any further.

3.1.2. Orientation dependence of integrated intensity (ODIN)

For realising a study with a great number of crystal orientations in a limited beam time we made use of an abbreviated method [29] which does not follow the decay of the NRS intensity over a longer time interval, but rather time-integrates over the intensity. For the method the name ODIN (orientation dependence of integrated intensity of NRS) was adopted. The idea is: a diffusionally accelerated decay will lead to a lower integrated intensity during the measuring period (about 165 ns after every pulse) than without diffusion. If the decay is purely exponential in time, as expected for a sufficiently thin sample, the integrated intensity depends in a simple way on the jump function $\alpha(\mathbf{Q})$, or – in other words – it is related in a simple way to the diffusional broadening of classical QMS:

$$I_{\mathrm{ODIN}}(\mathbf{Q}) = \int_0^\infty \mathrm{d}t\, I_{\mathrm{FS}}(\mathbf{Q},t) \propto \big(\Gamma_0+\Gamma_{\mathrm{d}}(\mathbf{Q})\big)^{-1}. \tag{3.6}$$

For FeAl we know from the earlier measurements [20,21] that in the limit of resolution the jumps are on Bravais lattices.

Figures 3 and 4 show ODIN values measured at 1030 °C, with the sample oriented in 44 different directions, together with model calculations. Because of experimental limitations the time integration was, of course, not from zero to infinity, but rather over a time window from 2 ns to 165 ns after the synchrotron pulse. This leads to a modification of eq. (3.6) by a factor which is a simple function of the period after the synchrotron pulse during which the time window is open.

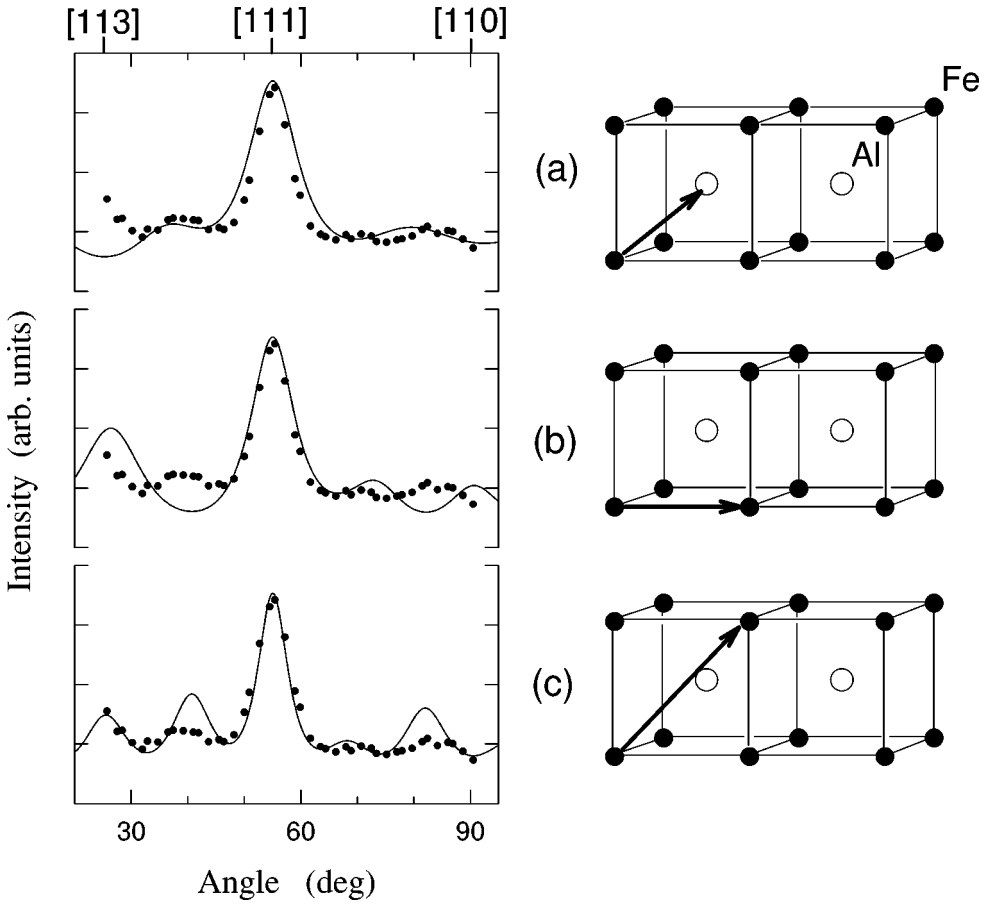

Figure 3. Orientation dependence of time-integrated intensity of delayed counts. Symbols: measured data. Lines: expected orientation dependence for three different types of jumps: (a) [1/2 1/2 1/2] – jumps of the iron atom into nearest neighbour sites, (b) [1 0 0] – jumps into second nearest neighbour sites, (c) [1 1 1] – jumps to third nearest neighbours.

In the figures a clear angular dependence is obvious. In the following we compare the data with expectations from different jump models. If there are several j independent jump paths, the diffusional line broadening $\Gamma_{\mathrm{d}}(\mathbf{Q})$ – and therefore also the ODIN value – is

$$I_{\mathrm{ODIN}}(\mathbf{Q}) \propto \big(\Gamma_0 + \Gamma_{\mathrm{d}}(\mathbf{Q})\big)^{-1} = \left[\Gamma_0 + \frac{2\hbar}{\tau}\sum_j W_j \alpha_j(\mathbf{Q})\right]^{-1}, \qquad (3.7)$$

where W_j are the probabilities for particular jump paths and $\alpha_j(\mathbf{Q})$ are the corresponding jump functions.

A comparison with the experimental data proves that the best fit (figure 4) is achieved with a combination of [1 1 0] and [1 0 0] jumps in the ratio of $(1.9 \pm 0.1) : 1$. These are jumps to sites on the iron sublattice of the ordered structure. Within errors the

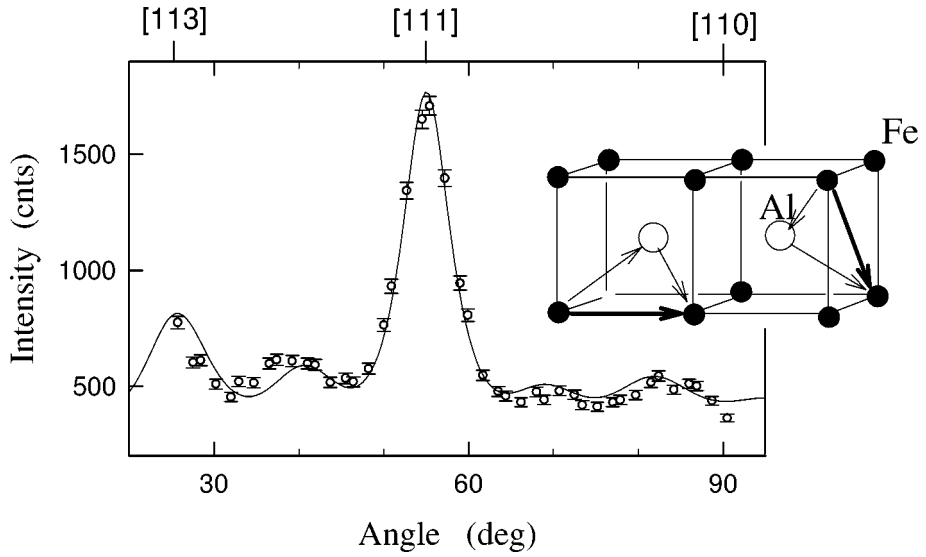

Figure 4. Orientation dependence of time-integrated intensity of delayed counts together with a model for a combination of [1 0 0] and [1 1 0] jumps via a short-time occupation of an antistructure site.

result agrees with conventional QMS [20], but the uncertainty of the NRS measurement is considerally smaller. The reasons are: Firstly, the angular resolution of NRS (μrad) is far better than that of QMS (0.12 rad). Secondly, such a dense chain of measurements as in figures 3 and 4 would need months in classical QMS (with NRS it needed about one hour); to keep the parameters constant and the sample composition and crystallinity stable at high temperatures (single crystal close to melting point!) is very difficult during such a long period.

The crystal structure of FeAl is that of ordered CsCl (B2) structure. The intriguing question how diffusion proceeds in such an ordered structure, where the nearest neighbours are of the other kind, has been under discussion for a considerable time.

Now from the described experiment, the *apparent* elementary diffusion jumps in FeAl are between sites on the iron sublattice without making use of the sites on the aluminium sublattice. All considerations regarding the underlying mechanism that lead to the measured combination of [1 1 0] and [1 0 0] jumps lead to the conclusion that a nearest neighbour *jump to an antistructure site on the Al sublattice* must be the elementary jump (see figure 4, inset). Even though that antistructure site must be occupied for a much shorter time than the "normal" positions on the iron sublattice, and therefore inaccessible to the earlier QMS measurement. It should form the basis for further jumps to second nearest neighbours, i.e., along [1 0 0] or to third nearest neighbours, i.e., along [1 1 0].

Calculations have been performed to explain the experiments and prove the basic mechanism. Questions addressed are: is the [1 1 0] preference a normal statistical effect or does it need coupled vacancies? Monte-Carlo calculations [22,23] appear to indicate the former: elementary jumps lead "automatically" to preference of neighbour

sites along [1 1 0] over sites along [1 0 0]. A disturbing issue results from first principle calculations [24] that find the jump to the antisite to be very costly in energy. Thus there remains a controversy on the details of the jump mechanism: is it really via the short-time residence on an antistructure site [25]?

It is challenging to find jumps to the antistructure site. We need to find a second component in the spectra attributable to fast jumps away from the antisite. Since that component's contribution would be small, QMS is not sensitive enough for a clear answer; we expect to obtain it from NRS with its considerably higher statistical precision and angular resolution.

3.2. Iron diffusion in Fe_3Si

Fe_3Si is another intermetallic alloy with ordered lattice structure. The first full report [18] on a measurement of diffusion in a crystal with the new technique of NRS of synchrotron radiation has been on this system.

For Fe_3Si the theory is slightly more complicated, since here we have three iron sublattices. Now the jumps between sites on the different sublattices (between sites on a non-Bravais lattice) are accessible to the measurements, we therefore expect several components in the spectra.

As in the preceding section, we have to find the intermediate scattering function and introduce it into eq. (2.5) in order to find the intensity of the forward scattered radiation. For diffusion via several sublattices of a non-Bravais lattice the intermediate scattering function is a sum over the sublattices [26,27]:

$$I(\mathbf{Q},t) = \sum_p w_p \exp\bigl[tM_p(\mathbf{Q})\bigr], \tag{3.8}$$

with $M_p(\mathbf{Q})$ the pth eigenvalue of the jump matrix $\mathbf{A}$ (the non-Bravais-lattice analogue to the jump function for a Bravais lattice) [18] and $w_p(\mathbf{Q})$ the weight of the component in the measured spectra corresponding to the pth eigenvalue of the jump matrix. The elements of the jump matrix $\mathbf{A}$ specify the various allowed jumps for the diffusing atom and the accompanying jump rates. In terms of QMS $M_p(\mathbf{Q}) = -\Gamma_{\mathrm{d},p}(\mathbf{Q})/2\hbar$, the negative value of the half width at half maximum of the diffusional part of the Mössbauer line.

In the case of Fe diffusion in Fe_3Si we deal with the so-called $D0_3$ lattice structure (figure 5), the superlattice is built up of four interpenetrating f.c.c. sublattices with three of them occupied by iron atoms (called α_1, α_2 and γ) and the fourth (called β) by silicon. The two α sublattices have different symmetries for γ- and β nearest-neighbours (NNs), iron atoms on α-sublattice sites with four iron NNs on γ-sublattice sites, iron atoms on γ-sublattice sites with eight iron NNs on α-sublattice sites. In earlier Mössbauer work it was proved that for stoichiometric composition a simple diffusion model with NN jumps of iron atoms between α- and γ-iron sublattice sites is sufficient [28].

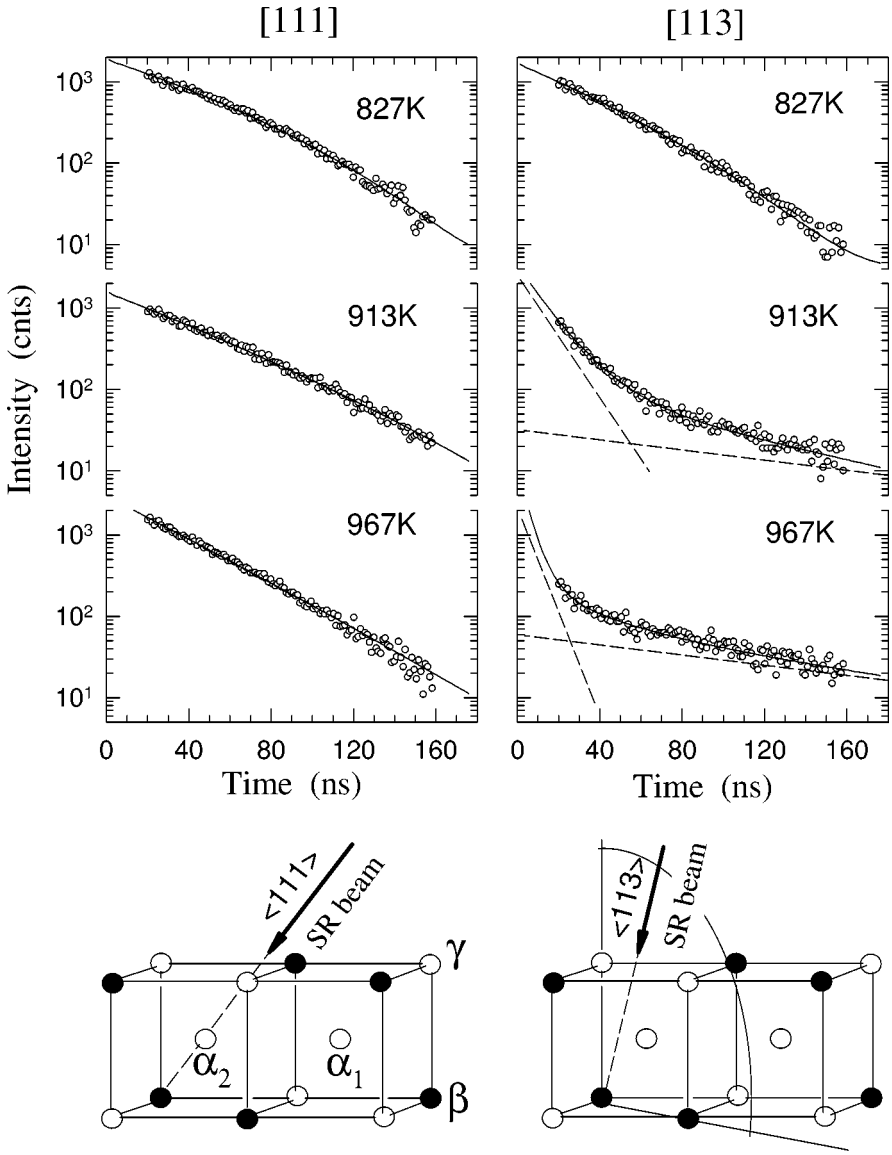

Figure 5. Fe_3Si. Top: time dependence of forward scattering intensity with the synchrotron beam along the [1 1 1] and [1 1 3] directions at three different temperatures. Bottom: 2/8 of elementary cell of the $D0_3$ structure. The iron atoms occupy the sublattices α_1, α_2 and γ (open circles), the silicon atoms the sublattice β (full circles).

For a stoichiometric $D0_3$ structure the jump matrix **A** has the form [28]

$$\mathbf{A} = \frac{1}{\tau_{\alpha\gamma}} \begin{pmatrix} -2 & E & E^* \\ E^* & -1 & 0 \\ E & 0 & -1 \end{pmatrix}, \tag{3.9}$$

where $1/\tau_{\alpha\gamma}$ is the jump rate of the iron atom from a site on a α sublattice into a vacancy on any NN site on the γ sublattice and vice versa, and E is a function of the structure of the jump lattice (see [28]). The matrix tells us that in general there are three components in the spectra with three different eigenvalues M_p (for QMS corresponding to three diffusionally broadened lines) with corresponding weights.

With **Q** parallel to special crystal directions, the number of components can be less than three: there are only two components when **Q** is parallel to a [1 1 3] crystal direction and only one for a [1 1 1] direction.

Single crystalline samples were measured in several orientations, in particular with the [1 1 3] and the [1 1 1] crystal directions parallel to the synchrotron beam.

Analytical calculations prove that in the [1 1 3] direction (only two components, the third has weight zero) the eigenvalues and relative weights for the slow component are very close to zero (no diffusional acceleration) and to $1/9$, for the fast component close to $3/\tau_{\alpha\gamma}$ and $8/9$, respectively. It is easily shown by numerical calculations (see, e.g., [10]) that in the thin sample approximation the decay of the forward scattered intensity can be approximately described by two exponentials, one of which exhibits the natural decay rate of the nuclear excitation while the other shows a diffusionally accelerated decay. The exact result is obtained by inserting the intermediate scattering function eq. (2.2) into the universal resonance function eq. (2.3) and the result into eq. (2.6).

Figure 5 shows time spectra – forward scattered intensity as a function of delay after the SR pulse – for both sample orientations and at two and three different temperatures. Whereas for the [1 1 1] orientation the decay is close to one exponential (non-accelerated), for the [1 1 3] orientation the time dependence may indeed be approximated by *two* exponential decays (dashed lines). The exact interpretation made use of convoluting with the Bessel function as a prefactor to follow the equation for non-infinitely thin samples. This correction, however, gives only a very slight bending down of the exponential functions. The results are in agreement, though not perfectly, with the simple theory. For more details on experiment and complete interpretation see [29].

The experiment was a feasibility test of a rather involved system – two different elementary jumps – and was not expected to provide results beyond what had been known from QMS. The elementary jump mechanism of the iron atoms is a to-and-fro jumping between α and γ sublattices avoiding the Si-sublattice.

3.3. A side-glance at diffusion in glasses

Meyer et al. [24] have undertaken NRS measurements in the forward direction on ferrocene/dibutylphthalate in the temperature range from 140 to 205 K, i.e., up to the glass transition in order to study relaxation. Whereas in the above described studies on crystalline materials NRS has no competition (except from the related methods of QMS and QNS), since other methods are completely unable to determine the *elementary jump, i.e., jump vector and frequency*, in glasses the aim is to determine relaxation

times which can also be drawn from a number of other methods. Nevertheless, Meyer et al. were able to demonstrate that in the future it should be possible with NRS to gain results competitive with or even superior to the wealth of already existing data, if one makes use of the unique features of SR, i.e., short measuring times, indispensable for the unstable glasses in particular near the glass transition, a narrow beam with small divergence, permitting the study of small samples. For details see Franz et al. [1].

4. Conclusions

In conclusion we state that it is possible to follow diffusion in the time domain by observing the diffusional acceleration of the intensity decay of nuclear resonant scattering (NRS) of synchrotron radiation in the forward direction, in analogy to conventional quasielastic Mössbauer spectrocopy (QMS) or quasielastic neutron scattering (QNS), both in the energy domain.

Definite advantages of the NRS method are:

(a) The highly brilliant synchrotron beam with its size of less than 1 mm^2 at the sample position and a divergence in the μrad range permits measurements of diffusional line broadening with considerably higher resolution.

(b) The narrow beam will enable diffusion investigations of small crystals and recrystallized foils.

Drawbacks of NRS for diffusion studies are:

(a) Presently, NRS is limited to moderately fast diffusion, since diffusivities higher than 10^{-12} m^2s^{-1} (corresponding for QMS on ^{57}Fe to diffusional line broadening of about 2 mms^{-1}) leads to a diffusional acceleration of the intensity decay within the dead time of the detection system of about 20 ns when using the intensity available at the ESRF for measurements of this kind. One can overcome this problem by sufficiently reducing the beam intensity, but, of course, pays for this with longer measuring times. One may hope for a reduction of the deadtime by an improvement of the electronics.

(b) An essential trivial drawback of NRS for diffusion studies compared to conventional Mössbauer studies in one's own laboratory should also be mentioned: the limited access (at least presently) to synchrotrons of the third generation for such studies.

Acknowledgements

The authors appreciate the very valuable discussions with G.V. Smirnov, V.G. Kohn, W. Petry, A. Meyer, H. Franz and R. Rüffer and the help of M. Kaisermayr in preparing essential parts of this manuscript. This work was supported by grants from the Austrian FWF (project No. S5601).

References

[1] H. Franz, A.Q.R. Baron and W. Petry, this issue, section V-2.1.
[2] N. Brockhouse, Nuovo Cim. Suppl. 9 (1958) 45; Phys. Rev. Lett. 2 (1959) 287.
[3] R.C. Knauer and J.G. Mullen, Phys. Rev. 174 (1968) 711.
[4] K.S. Singwi and A. Sjölander, Phys. Rev. 119 (1960) 863; Phys. Rev. 120 (1960) 1093.
[5] E. Gerdau, R. Rüffer, H. Winkler, W. Tolksdorf, C.P. Klages and J.P. Hannon, Phys. Rev. Lett. 54 (1985) 835.
[6] E. Gerdau and U. van Bürck, in: *Resonant Anomalous X-Ray Scattering. Theory and Applications*, eds. G. Materlik, C.J. Sparks and K. Fischer (Elsevier, Amsterdam, 1994) p. 589.
[7] G.V. Smirnov, Hyp. Interact. 97/98 (1996) 551.
[8] C.T. Chudley and R.J. Elliott, Proc. Phys. Soc. London 77 (1961) 353.
[9] G.V. Smirnov and V.G. Kohn, Phys. Rev. B 52 (1995) 3356.
[10] V.G. Kohn and G.V. Smirnov, Phys. Rev. B 57 (1998) 5788.
[11] U. Bergmann, J.B. Hastings and D.P. Siddons, Phys. Rev. B 49 (1994) 1513.
[12] A. Meyer, H. Franz, J. Wuttke, W. Petry, N. Wiele, R. Rüffer and C. Hübsch, Z. Phys. B 103 (1997) 479.
[13] G. Vogl, B. Sepiol, H. Thiess and M. Kaisermayr, ESRF report HS-584 (1999).
[14] V. Smirnov, U. van Bürck, A.I. Chumakov, A.Q.R. Baron and R. Rüffer, Phys. Rev. B 55 (1997) 5811.
[15] A.Q.R. Baron, H. Franz, A. Meyer, R. Rüffer, A.I. Chumakov, E. Bürkel and W. Petry, Phys. Rev. Lett. 79 (1997) 2823.
[16] K. Ruebenbauer and U.D. Wdowik, Phys. Rev. B 58 (1998) 11896.
[17] R. Rüffer and A.I. Chumakov, Hyp. Interact. 97–98 (1996) 509.
[18] B. Sepiol, A. Meyer, G. Vogl, R. Rüffer, A.I. Chumakov and A.Q.R. Baron, Phys. Rev. Lett. 76 (1996) 3220.
[19] B. Sepiol, C. Czihak, A. Meyer, G. Vogl, J. Metge and R. Rüffer, Hyp. Interact. 113 (1998) 449.
[20] G. Vogl and B. Sepiol, Acta Metall. Mater. 42 (1994) 3175.
[21] R. Feldwisch, B. Sepiol and G. Vogl, Acta Metall. Mater. 43 (1995) 2033.
[22] R. Weinkamer, P. Fratzl, B. Sepiol and G. Vogl, Phys. Rev. B 58 (1998) 3082.
[23] R. Weinkamer, P. Fratzl, B. Sepiol and G. Vogl, Phys. Rev. B 59 (1999) 8622.
[24] J. Mayer and M. Fähnle, Defect and Diffusion Forum 143–147 (1997) 285.
[25] G. Vogl, B. Sepiol, C. Czihak, R. Rüffer, R. Weinkamer, P. Fratzl, M. Fähnle and B. Meyer, Mat. Res. Soc. Symp. Proc. 527 (1998) 197.
[26] J.M. Rowe, K. Sköld, H.E. Flotow and J.J. Rush, J. Phys. Chem. Solids 32 (1971) 41.
[27] O.G. Randl, B. Sepiol, G. Vogl, R. Feldwisch and K. Schroeder, Phys. Rev. B 49 (1994) 8768.
[28] B. Sepiol and G. Vogl, Phys. Rev. Lett. 71 (1993) 731.
[29] B. Sepiol, A. Meyer, G. Vogl, H. Franz and R. Rüffer, Phys. Rev. B 57 (1998) 10433.